Nitrogen oxides and ozone production in the North Atlantic marine boundary layer

Thomas P Carsey, Dean D Churchill, Michael L Farmer, Charles J Fischer, Alexander A Pszenny, Victor B Ross, Eric S Saltzman, M. Springer-Young, Bernard Bonsang

JOURNAL OF GEOPHYSICAL RESEARCH, VOL. 102, NO. D9, PAGES 10,653–10,665, MAY 20, 1997

Nitrogen oxides and ozone production in the North Atlantic marine boundary layer

Thomas P. Carsey,[1] Dean D. Churchill,[2] Michael L. Farmer,[1] Charles J. Fischer,[1] Alexander A. Pszenny,[3] Victor B. Ross,[4] Eric S. Saltzman,[2] M. Springer-Young,[1] and Bernard Bonsang[5]

Abstract. Measurements of reactive nitrogen gases (NO, NO_2, NOy), as well as related chemical (O_3, CO, aerosol black carbon, radon, selected nonmethane hydrocarbons) and meteorological parameters were made on board the R/V *Malcolm Baldridge* prior to and subsequent to the 1992 ASTEX (Atlantic Stratocumulus Transition Experiment) in the North Atlantic Ocean during June and July 1992. Results showed indications of well-defined plumes from North America and Europe from both chemistry and back trajectory data. Elevated ozone concentrations were also observed in airmasses from uninhabited continental regions. Chemical and meteorological data were incorporated into a simple photochemical model in which ozone destruction predominated over generation. The principal reaction leading to ozone destruction was $O(^1D) + H_2O \rightarrow 2OH$.

Introduction

There has been a sustained interest in understanding the biogeochemical role of tropospheric active nitrogen gases such as nitric oxide (NO) and nitrogen dioxide (NO_2), due to their role in the control of ozone production during hydrocarbon oxidation [*Crutzen*, 1970]. There is general agreement that the mixing ratio of NOx in a large portion of the marine boundary layer is near or below the threshold for ozone production during hydrocarbon oxidation [e.g., *Liu et al.*, 1987; *Chameides et al.*, 1987; *Thompson et al.*, 1993]. However, there remain gaps in our understanding of the odd nitrogen cycle in the marine troposphere [*Kasibhatla et al.*, 1993] due in part to the paucity of field data for the key chemical species [*Carney and Fishman*, 1986]. In this paper, measurements of NO, NO_2, their sum (denoted NOx) and NOy, along with ozone and carbon monoxide obtained during a cruise aboard the NOAA research ship *Malcolm Baldrige* during June 1992 are reported and interpreted in an effort to better understand the role of terrestrial gases in the marine boundary layer, specifically with respect to the effect of limited odd nitrogen concentration on ozone production and destruction. The cruise was organized as a component of the 1992 Atlantic Stratocumulus Transition Experiment (ASTEX) program and was additionally sanctioned by the Marine Aerosol and Gas Exchange (MAGE) project within the International Global Atmospheric Chemistry Program (IGAC).

[1]National Oceanic and Atmospheric Administration, Atlantic Oceanographic and Meteorological Laboratory, Miami, Florida.

[2]Rosenstiel School of Marine and Atmospheric Science, University of Miami, Miami, Florida.

[3]International Global Atmospheric Chemistry Program Office, Department of Chemistry, Massachusetts Institute of Technology, Cambridge.

[4]Naval Oceanographic Office, Stennis Space Center, Mississippi.

[5]Centre National de la Recherche Scientifique, Centre des Faibles Radioactivités, Gif sur Yvette, France.

Paper number 96JD03511.
0148-0227/97/96JD-03511$09.00

Experimental Methods

Measurements of a number of significant trace gases and aerosol species were obtained on board the ship. The relevant portion of the cruise track is shown in Figure 1. Gaseous analytes species (with abbreviations used below) include ozone (O_3), carbon monoxide (CO), black carbon (BC), radon 222 (Rn), nitric oxide (NO), nitrogen dioxide (NO_2), and reducible reactive nitrogen gases (NOy).

Nitrogen Oxides

Nitrogen oxides were measured by a chemiluminescence instrument according to established protocols [e.g., *Ridley*, 1978; *Carroll et al.*, 1985]. Air inlets for NO, NO_2, and NOy, along with the NO_2 permeation device, NOy converter and various Teflon® valves (Delta; Gulf Technical Service) were housed in a sampling box suspended on a cable running from the air-sampling van to a 10-m atmospheric sampling tower mounted on the bow of the ship. The sampling box was kept at a distance of about 5 m from the van in order to avoid possible pollution from operations on the ship, while allowing for short sampling lines. This sampling box was plumbed to allow NO and NO_2 calibration gases to be inserted into the sampling line at a minimum distance downstream of the inlet filters. NO_2 calibrate gas was also directed into the NOy sampling line to provide a check on the conversion efficiency throughout the cruise. To avoid contamination by sea-salt aerosols, each sampling line was capped by a 37-mm-diameter 1-μm pore size Teflon filter (Gelman). Conversion of NO_2 into NO for chemiluminescence detection was accomplished within a 0.8-L

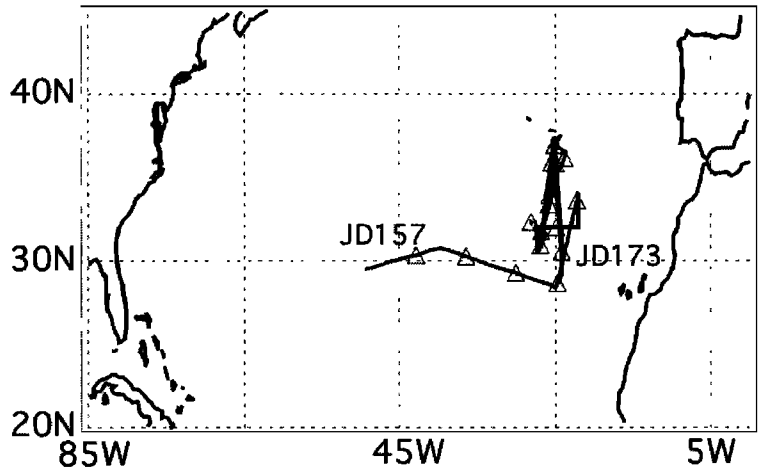

Figure 1. Cruise track of the 1993 R/V *Malcolm Baldrige* cruise MB-92-03-ASTEX, portion from JD 156 (June 4, 1992), 29°30'N/49°20'W, through JD 174 (June 22, 1992), 28°24'N, 24°54'W. Ship positions at the beginning of each Julian day are indicated by a triangle.

photolysis chamber illuminated by a 300 W Xenon lamp (ILC Technology). The upbeam end window was a 3-inch-diameter Pyrex disk (Esco Products); the downbeam end of the chamber was made from a 3-inch-diameter parabolic mirror (Edmund Scientific) coated for ultraviolet reflection (Al-MgF_2 film, Evaporated Metal Films, Ithaca, New York). The cell was designed to have uninterrupted airflow at all times; for all measurements other than the NO_2 ambient read and NO_2 calibrate, a motor-driven shutter system was employed to block the light path. Thus, for the NO_2 blank measurement, the door would be closed; however, a noise spike from an undetermined source voided many NO_2 blank determinations. In those cases the NO ambient read was used for the NO_2 blank rate; in cases where the shutter-closed reading was available, no difference was seen in the ambient NO_2 determination using the two methods. Overall efficiency of the cell was monitored throughout the cruise; average efficiency was 88%. For NOy, a molybdenum converter was used for reduction of NOy species to NO [*Joseph and Spicer*, 1978; *Fehsenfeld et al*, 1987]. The airstream was passed over 8 g molybdenum wire (0.05 mm diameter) packed in 6 inch × ¾ inch stainless steel tubing temperature controlled (Thermologic) to 400°C. This unit was placed near the sample box inlet to minimize loss of nitric acid. In order to protect the unit from marine aerosols, the air first passed through a 1-μm pore size Teflon filter. Thus, aerosol nitrate was not reduced by the converter; NOy as measured with this instrumentation did not include nitrate. The converter system was evaluated in the laboratory prior to the cruise, where quantitative conversion of NO_2 was observed. Air for all three chemiluminescence analytes (NO, NO_2, NOy) was routed from the box to the van through one sample line; this arrangement has been found to reduce variations in the background count rate. For NO and NOy analysis, the pressure drop in the lines and reaction vessel was controlled by a flow-limiting critical orifice (1.1 L min^{-1}) in the sampling box directly downstream of the inlet filter. Thus the line was held at reduced pressure (6.9 torr inside the reaction chamber) and travel time for the gas to the reaction chamber was estimated to be less than 1 s. For NO_2 analysis, the orifice was bypassed and the flow and pressure drop were controlled by a mass flow controller downstream of the photolysis chamber; photolysis took place near atmospheric pressure and a flow of 1.24 L min^{-1}. Chemiluminescent emission was recorded by a 9658R photomultiplier tube (Thorn EMI) held at 1450 V and housed in a cooled housing (Products for Research) maintained at -40°C. The housing assembly was mated to an internally gold coated stainless steel reaction vessel (design courtesy of B. Ridley) by an interface of our design containing a UV filter (Schott RG610). Instrument control and data acquisition were performed via a computer employing Labtech® software and Metrabyte® component boards. A timing cycle of ~50 min duration was used which included blank, ambient, and calibration intervals for all three analytes. Photon counts were recorded every 10 s during the cycle. The first 3-4 min of each interval were ignored to allow the system to equilibrate (first 1 min for NO). The data were scanned for spikes or other anomalies due to other shipboard instrumentation; questionable 10-s counts were deleted. Remaining counts from each interval were then converted into count rates (counts per second). For NO, the blank rate was determined by passing the air through a 1-L prereaction unit which allowed mixing of NO and ozone prior to entrance into the reaction chamber. The NO_2 blank rate was taken to be the NO ambient rate that would have been measured at the time the NO_2 ambient rate was obtained; this was calculated by a linear interpolation of two NO ambient rates obtained before and after the NO_2 rate. An analogous interpolation was used to estimate the NOy blank rate from two NO blank rates. This approach was employed to minimize the effect of drift in the instrument performance during the run. For all analytes, obvious outliers were deleted. For NO_2, a correction was applied to remove NO_2 estimated to be produced from NO by ambient ozone prior to analysis. Subsequent to the cruise, it was noted that there was a significant baseline drift in the data, especially after June 21 (Julian day (JD) 173); data after JD 173 were disregarded. The drift may have been due to residual gases in the sample lines following aft winds or to diurnal changes in reaction chamber temperature

which could not always be adequately removed by the above algorithm. For each analyte, the two rates in each cycle were converted to concentrations and averaged; these values were subjected to a running five-point (~4 hour) average to reduce the noise. Finally, nonzero nighttime NO concentrations were assumed to be instrumental error and were subtracted from the daytime concentration. The sensitivities (counts per second per parts per trillion) of the instrument were determined by standard techniques. For NO, a commercial calibration gas mixture (123 ppbv NO in N_2, Scott Specialty Gas) was injected into the inlet stream. For NO_2 and NOy, an 80 cm^3 min^{-1} N_2 gas stream which passed over an NO_2 permeation device (VICI Metronics) housed in an insulated chamber held at 30°C (Thermologic) was added to the ambient airstream. The permeation rate of the device was determined from gravimetric analysis of the device over a period of 16 months to be -9.78 ng min^{-1}, in approximate agreement with the manufacturer's specification of -10 ng min^{-1}. Calibrations were done for each analyte on each cycle. Average sensitivities during most of the cruise were 5.38 cps ppt $^{-1}$ for NO; 5.47 cps ppt $^{-1}$ for NOy; and 4.46 cps ppt $^{-1}$ for NO_2. Measured sensitivities varied a few tenths counts per second per parts per trillion around these means; excursions were generally related to temperature changes inside the equipment or to gas contamination from the ship. The lower limit of detection of the instrument due to count rate error [*Jenkins,* 1978] was ~3.0 ppt for NO and NOy, and ~3.7 ppt for NO_2. For all analyses, blank values of ~2000 cps produced random errors (2σ) of ~13% [*Jenkins,* 1978]; total error including instrumental drift was estimated to be 40% [*Carroll et al.,* 1985]. The instrument was intercompared with two other instruments in 1994 (T. Carsey, manuscript in preparation, 1996). An intercomparison of three chemiluminescence instruments including the author's was made at Harvard Forest during 1994. Instrument errors were subsequently found in the author's calibration system and the data were recomputed using new standards. Reduced major axis comparison [*Sokal and Rohlf,* 1981] of the results obtained slopes of 0.993 (r = 0.989) and 0.913 (r = 0.965) of the author's NO data compared to the other two instruments. The results are in preparation for publication.

Carbon Monoxide

Carbon monoxide (CO) was sampled by hand-held gas syringe at various places on the forward deck of the ship, 9 m to 12 m above sea level; no difference was noted which could be ascribed to sampling location. The sampled air was injected into a Carle Model 400 gas chromatograph with an RGD2 HgO gas reduction detector (Trace Analytical, Inc., Menlo Park, California), as described by *Piotrowicz et al.* [1990]. Calibrations were performed daily; however, day-to-day changes were so minor that a single calibration curve was applicable to the entire data set. Instrument variance (pooled) was 2-4 ppb; accuracy was estimated to be within 5%.

Ozone

Ozone was measured by a Dasibi model 1008-AH ozone analyzer and by an Environics Series 300 unit, both operating continuously. The Dasibi unit was mounted aft of the bridge connected to an 8-m Teflon sample line with an inlet ~46 m above the sea surface; the second unit was located on the forward main deck with 9-m Teflon sample lines with an inlet approximately 10 m above the sea surface. Sample lines were protected from aerosols by a 20-μm pore size 47-mm-diameter Teflon filter (Savillex Corporation, Minnetonka, Minnesota). Baseline readings were determined daily by passing the air stream through Hopkalite®. Both instruments gave results which did not differ significantly; mean difference between June 3 and June 21 was 0.04 ppbv. The ozone analyzers were calibrated prior to the cruise according to Environmental Protection Agency protocols by the Dade County, Florida, Department of Environmental and Resource Management; both instruments were accurate to <1%; precision was <0.5% relative standard deviation at 100 ppb.

Aerosol Black Carbon

Black carbon was measured with an aethalometer [*Hansen et al.,* 1990] set to take readings at 5-min intervals. Air was fed to the instrument at 20±1 standard liters per minute (SLPM) through approximately 10 m of polypropylene tubing suspended on a cable running from the air-sampling van to the bow tower. The inlet of the tubing was at approximately 16 m above sea level, 10 m aft of the forward bulwark, and was fitted with a rain shield made from a 125-mL polyethylene bottle from which the bottom had been removed. Raw data were recorded on a computer. The four light attenuation data series were smoothed individually using a nine-point moving average, and these smoothed values were then used in the algorithm supplied by the instrument manufacturer (Magee Scientific, Inc.) to calculate black carbon concentrations. A value of 19 m^2 g^{-1} was used for the specific attenuation of black carbon on the quartz fiber filters used (Pallflex Tissuequartz 2500 QAT-UP). The active collecting area of filter was 0.9 cm^2. The filter was replaced at least once per day. The precision, based on variance of the blanks, was 5%; accuracy was estimated at 10% [*Hansen et al.,* 1990].

Radon

Radon 222 was estimated indirectly via assay of its short-lived, β particle emitting daughters (^{214}Pb and ^{214}Bi) in aerosols with a system based on the design of *Larson and Bressan* [1978]. Air was drawn through a 10-cm-diameter glass fiber filter (Schleicher and Schuell, number 29) for the first 20 min of an 80-min cycle at a flow rate of 0.7 m^3 min^{-1}. Beta particles were then counted during four 10-min intervals beginning at 1, 11, 40, and 50 min after pumping stopped. The detector was a plastic scintillator (Nuclear Enterprises, Inc., San Carlos, California, model NE 102A) optically coupled to a photomultiplier tube (Amperex model XP2202 B/06). The detector face was centered approximately 1.5 cm from the filter surface and was shielded from visible light by covering it with Al foil (5 mg cm^{-2}). The filter-detector assembly was housed in a box secured on deck outside the air sampling van. Variations in counting efficiency were checked by counting sources of ^{90}Sr-^{90}Y, ^{210}Pb-^{210}Bi, ^{36}Cl, and ^{99}Tc (Dupont NES-261, NES-200F, NES-200D, and NES-200-B, respectively) centered in fixed geometry in circular plastic frames that were placed individually in the filter holder for 2-3 min during the daily filter change interval. These data revealed a strong negative dependence of counting efficiency on temperature inside the box that housed the filter-detector assembly. Corrections were possible up to a box temperature of 30°C, but resulted in

uncertainties of approximately ±30% in estimated ^{222}Rn concentrations. Conversion of counting data to ^{222}Rn concentrations was based on *Bateman's* [1910] method. The detection limit for the system was estimated at 1 pCi m^{-3} [*Hansen et al.*, 1990].

Nonmethane Hydrocarbons (NMHCs)

Air samples for NMHC analysis were collected in 6-L stainless steel electropolished canisters, rinsed with UHP helium and evacuated while heated before sampling. Sampling occurred on the windward bow of the ship, at 20 m above the sea surface. To minimize concentration changes inside the canisters, the samples were cryogenically enriched immediately following the sampling and then analyzed by gas chromatography (Varian 3400) with a flame ionization detector. Helium used as carrier gas was purified with a charcoal trap maintained in liquid nitrogen prior to its introduction in the injection system. Sample fractions of 500-600 mL were drawn from the canisters and enriched in a first trap (1/8-inch OD × 25 cm) filled with Tenax GC and cooled to -120°C with an ethanol/liquid N_2 mixture. The flow rate through this trap was 50 mL min^{-1}; the trap had been previously shown to quantitatively retain C_2-C_6 hydrocarbons at this rate. After purging the trap with the UHP helium, the sample was thermodesorbed and transferred under the helium stream to a U-shaped loop (1/16-inch OD) filled with glass beads, cooled in liquid N_2 and connected to the head of the column. The injection was then performed by quickly heating this trap to 95°C in a hot water bath. Separation was obtained through a 50-m-length, 0.32-mm-ID, Al_2O_3/KCl porous layer open tubular column (Chrompack). The column temperature program was 40°C for 0.5 min and then increased to 120°C at 25°C min^{-1}. Before each enrichment step, the Tenax trap was carefully cleaned in the UHP helium stream. Blank measurements were performed twice a day in order to check the absence of memory effect in the traps as well as the purity of the carrier gas. Calibrations were performed daily from a reference standard prepared by static dilution and injected with a "Pressure Lok" syringe. The detection limit was estimated to be 5 pptv for C_2 to C_6 hydrocarbons. The accuracy of the analysis was typically of the order of 5% for sub-part-per-billion-by-volume levels of hydrocarbons.

Back Trajectories

During leg 1 of the cruise, rawinsondes were launched every 3-4 hours. These data were forwarded to NOAA Environmental Research Laboratory along with other appropriate meteorological data and included as parameterization for the hybrid single-particle Lagrangian integrated trajectories (Hy-Split) model [*Draxler*, 1992]. The model was then run to generate back trajectories at the location of the ship and at terminal altitudes of 1 km and 2 km, taken to represent the top of the marine boundary layer as interpreted from rawinsonde data.

Results

The concentrations of NO, NO_2, NOy, O_3, CO, Rn, and BC are presented in Figure 2 for the period June 4 through June 21, 1992. Initially, the sources for air sampled during this time were interpreted on the basis of Rn/BC ratios, as suggested by *Hansen et al.* [1990], and back trajectory calculations. Aerosol BC is considered to be produced in significant quantities only by combustion processes [*Goldberg*, 1985], while Rn is released almost entirely by soils [*Wilkening and Clements*, 1975]. Visual examination of the data suggested four types of source definitions: inhabited continental (high BC and Rn); uninhabited continental (high Rn, low BC); mixed marine and continental air; and clean marine air (low BC and Rn); these are denoted I, U, M and C, respectively, in the discussion below, and in Figure 3 and Table 1. Some short events were interpreted as locally contaminated marine air, i.e., plumes from passing ships or contamination from the *Baldrige* via wind turbulence (high BC,

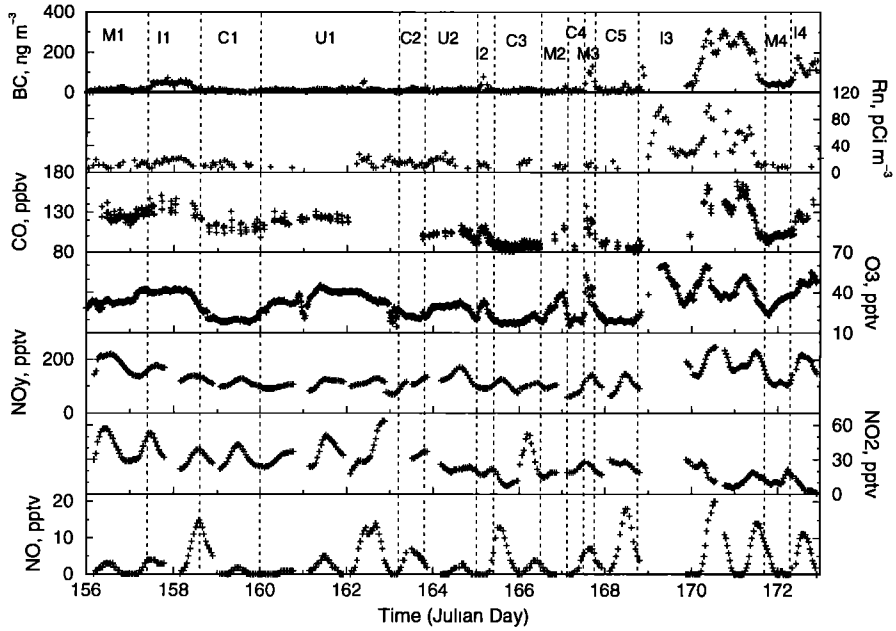

Figure 2. Results of analysis of air samples aboard the R/V *Malcolm Baldrige* during the 1992 ASTEX cruise. Dashed vertical lines separate airmass categories as described in the text.

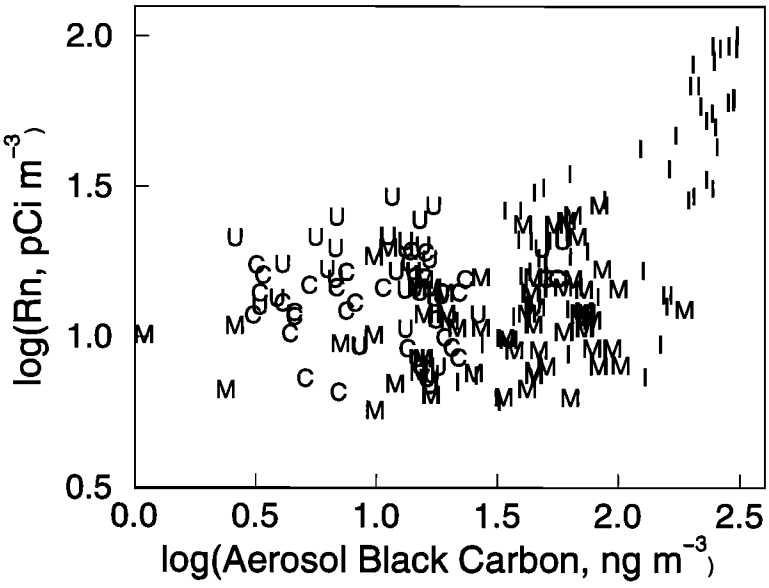

Figure 3. Log plot of near-simultaneous measurements of Rn and BC. Letter indicates the designated type of airmass (I=inhabited continental; U=uninhabited continental; C=clean marine air; M=mixed marine and continental air).

low Rn). The above categories are perforce inexact and are used for descriptive purposes only.

Clean Marine Air (C)

Six episodes of relatively clean marine air were identified. Levels of O_3, Rn, and CO were characteristically low (Table 1) although some degree of terrestrial input was generally observed. The average ozone mixing ratio of 21 ppbv is within the range reported by *Winkler* [1988] and compares generally with that of 10-20 ppbv reported by *Piotrowicz et al.* [1990]. Radon levels of 13 pCi m^{-3} are higher than those reported by *Hansen et al.* [1990], which may be due to instrumental problems described above. Average black carbon concentrations of 15 ng m^{-3} are comparable to those reported by *Hansen et al.* [1990], of 6-20 ng m^{-3}. Carbon monoxide mixing ratios averaged 95 ppbv for this category; for C3-C6 the average is 89.9 ppbv. These values compare well with the measurements of *Novelli et al.* [1992] for Mauna Loa Observatory for June (~80-105 ppb), and of *Doddridge et al.* [1994] from Mace Head, Ireland, for marine air. NO and NO_2 averages for 5 and 29 pptv (Table 1) were comparable to those reported by *Broll et al.* [1990] and *Rohrer and Brüning* [1992] in the North Atlantic. The former reported NO_2 at 50-90 pptv at ~38°N; the latter reported mixing ratios of 8-10 pptv for NO and 20-30 pptv for NO_2 at 30°N (latitude range reported here was ~29-35°N). Similarly, a range of nighttime NO_2 of ~30-90 pptv can be estimated for this latitude from *Broll et al.* [1990]. Back trajectory calculations for clean air episodes show the expected anticyclonic circulation, often within the marine mixed layer for most or all of the 10 days of the trajectory; an example is shown in Figure 4 for C1.

Uninhabited Continental (U)

Two episodes encountering air of uninhabited continental air were noted; the first from JD 160-163.2 (June 8-11), the second from JD 163.8-165 (June 8-9). The two episodes can be viewed as a single episode interrupted by a brief period of clean marine air (C2). The U designation is derived from the surface back trajectories, which indicate an origin in the Labrador/Greenland region 8-10 days prior to sampling, with upper level air descending in a southward track to the ship. U1 is shown in Figure 5; U2 is similar. Chemical signals include elevated Rn (average of 16 pCi m^{-3}), elevated O_3 (average of 32 ppbv), and somewhat elevated CO (average of 113 ppbv) levels, but without significantly elevated BC (average of 15 ng m^{-3}), compared to clean marine regions.

Inhabited Continental (I)

Four distinct episodes of air unambiguously identified with continental influence can be noted. The first, denoted I1, JD 157.4-158.6 (June 5-7), showed clearly enhanced concentrations of BC, Rn, CO, and O_3, and slightly higher NO_2 and NOy. Back trajectories for this episode show an origin in eastern Canada (Figure 6). A very brief episode, I2, occurred from JD 165.0 to 165.4 (June 13); back trajectories indicated input at the 2 km level. The third, I3, shown in Figure 7, JD 168.8-171.7 (June 16-19), is much more intense than I1, with very high concentrations of BC, Rn, CO, and O_3, and elevated concentrations of NOy (several instruments were off line during June 17). Back trajectories show the onset of this plume in the afternoon of June 16 (JD 168), when the winds became easterly and transport of heavily polluted air from Europe occurred in as little as 3 days. The episode is noted for large changes in all chemistries and simultaneously in the wind speed and direction as recorded on the ship. A sustained interruption of the plume by an intrusion of marine air occurred on the evening of June 19 (JD 172) which drove all measured concentrations almost to background levels. This intrusion event was assigned as a mixed air episode M4. Finally, episode I4 was noted (JD 172.3-174.5) with high levels of all measured components; the

Table 1. Measured Concentrations by Air Mass Category

Air Type	Sequence Number	Start Time, JD	End Time, JD	BC, ng m^{-3}	Rn, pCi m^{-3}	O_3, ppbv	CO, ppbv	NO, pptv	NO_2, pptv	NOy, pptv	Approximate Ship Location Start Latitude/Longitude	Approximate Ship Location End Latitude/Longitude
						Clean Marine Air						
C1	3	158.6	160.0	9±5	12±4	21±3	112±7	5±5	32±6	116±11	29°36'N 32°32'W	28°39'N 24°45'W
C2	5	163.2	163.8	15±6	13±4	23±1	100±3	5±2	34±2	114±11	36°56'N 25°09'W	35°02'N 25°12'W
C3	8	165.4	166.0	8±4	12	18±1	87±4	8±4	12±5	107±18	31°19'N 26°37'W	32°17'N 28°01'W
C4	10	167.12	167.5	11±6	-	11±24	86±78	3±2	22±3	76±14	29°03'N 24°27'W	35°19'N 24°40'W
C5	12	165.75	168.75	20±31	12±4	25±9	91±10	5±5	24±9	103±23	31°43'N 24°46'W	37°24'N 24°28 W
C6	17	177.8	178.6	31±19	13±4	20±4	91±2	3±2	66±14	15642	29°02'N 24°35'W	29°58'N 23°44'W
Average			16±22	15±4	23±8	94±8	5±4	29±8	111±21			
						Uninhabited Continental Air						
U1	4	160.0	163.2	15±8	16±6	35±6	122±4	5±4	35±11	106±17	28°39'N 24°46'W	36°56'N 25°09'W
U2	6	163.8	165.0	14±6	17±6	29±4	103±5	2±1	24±5	140±20	35°02'N 25°12'W	31°03'N 26°51'W
Average			15±7	17±6	33±5	113±5	4±4	33±10	114±18			
						Inhabited Continental Air						
I1	2	157.4	158.6	43±15	16±5	39±5	136±7	6±4	36±10	152±21	30°43'N 40°07'W	29°36'N 32°32'W
I2	7	165.0	165.4	30±22	12±3	25±7	101±7	3±2	19±2	97±3	31°03'N 26°51'W	31°19'N 26°37'W
I3	13	168.8	171.7	181±95	50±26	44±10	130±24	9±6	16±7	189±34	37°24'N 24°28'W	31°58'N 26°00'W
I4	15	172.3	174.5	127±33	25±11	41±5	121±10	11±10	19±7	253±81	32°00'N 23°10'W	27°23'N 25°03'W
Average			120±66	35±18	39±8	124±17	8±7	19±7	172±78			
						Mixed Marine and Continental Air						
M1	1	156.0	157.4	14±7	12±4	35±4	125±6	2±1	40±10	179±332	29°30'N 49°20'W	30°43'N 40°07'W
M2	9	166.5	167.12	11±10	9±2	31±9	104±7	2±1	17±2	101±5	31°05'N 27°17'W	34°03'N 25°27'W
M3	11	167.5	167.75	104±51	12±3	38±11	107±10	7±1	25±2	135±10	35°19'N 24°40'W	35°43'N 24°14'W
M4	14	171.7	172.3	43±5	10±3	35±5	100±4	4±3	13±4	119±16	31°58'N 26°00'W	32°00'N 23°10'W
M5	16	174.5	177.8	75±20	14±6	30±6	109±9	11±8	46±26	299±133	27°23'N 25°03'W	29°03'N 24°35'W
M6	18	178.6	181.0	40±15	12±6	28±6	97±4	5±4	35±20	166±96	29°58'N 23°44'W	36°38'N 24°33'W
Average			49±17	12±5	31±6	112±7	7±6	29±20	191±97			

Values are concentrations at ±1 standard deviationl JD denotes Julian day; BC denotes black carbon aerorol.

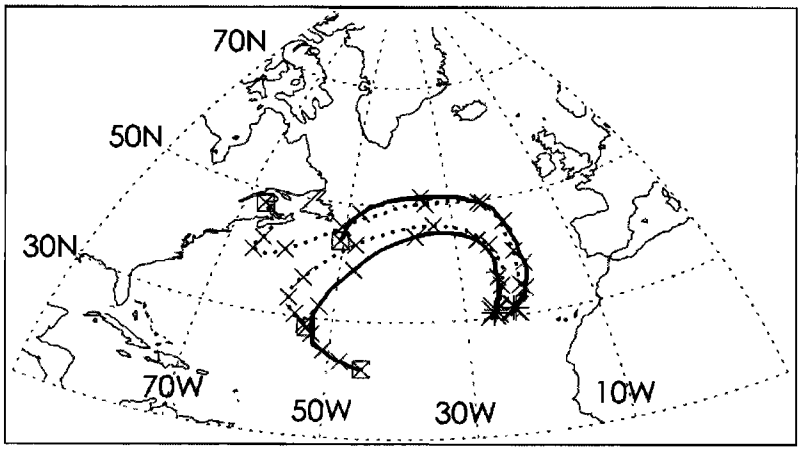

Figure 4. Ten-day back trajectories for days associated with C1 clean air episode, June 6 through June 7 (JD 158.6-160.0). Shown are two pairs of trajectories; each pair has one trajectory terminating at 2 km (dotted curve) and one at 1 km (solid curve). Points marked with a cross denote positions of the air parcel at 1-day backward intervals on both panels; the square denotes the origin of the trajectory. Westernmost terminus marks ship position at JD 159; easternmost is JD 160. Symbols and labels are continued in Figures 4 through 9.

back trajectories were similar to those of I3 at the beginning of the episode, with all trajectories terminating at 1 km or below passing over western Europe in the previous 3½-5 days. Around JD 176 (June 24), upper level trajectories indicate an origin in North America (Figure 8). Unfortunately, during most of I4 the ship was in port and thus fewer data were available for this episode.

Mixed Marine and Continental (M)

Six episodes of mixed air were encountered which were characterized by slightly elevated concentrations of most of the measured components and by back trajectories which at some level were traceable back to a continental landmass. The first, M1, JD 156.0-157.4 (June 4-5), was characterized by slightly elevated but rising O_3 and CO levels, anticipating episode I1 as well as elevated NOy and low BC and Rn. Back trajectories at 1, 2, and 3 km levels originated at or near the NE coast of the United States or from eastern Canada; the air had aged 9-10 days prior to its arrival above the ship. The second, M2, JD 166.0-167.12 (June 14-15), is unusual in that almost all back trajectories are over the ocean at all termination heights except for a few at high altitudes (3 or 4 km). Several spikes in BC, O_3 and CO were noted; however, NOy, NO_2, Rn and BC were low and mostly featureless. M3 is a brief episode of elevated chemistries which occurred at JD 167.6-167.75 (June 15) and was associated with upper air trajectories from North America. Episode M4 was previously noted as a marine air intrusion between I3 and I4. Episode M5, from JD 174.5-177.8 (June 22-25), was characterized by BC consistently higher than background levels and decreasing CO and O_3; the mixed nature of the back trajectories is indicated in Figure 9. The NOy

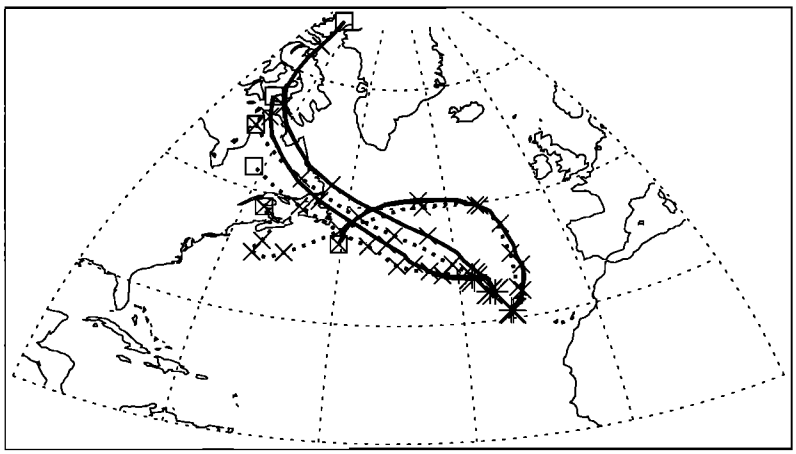

Figure 5. Ten-day back trajectories for days associated with U1 uninhabited continental episode, June 7 through June 11 (JD 160-163.2).

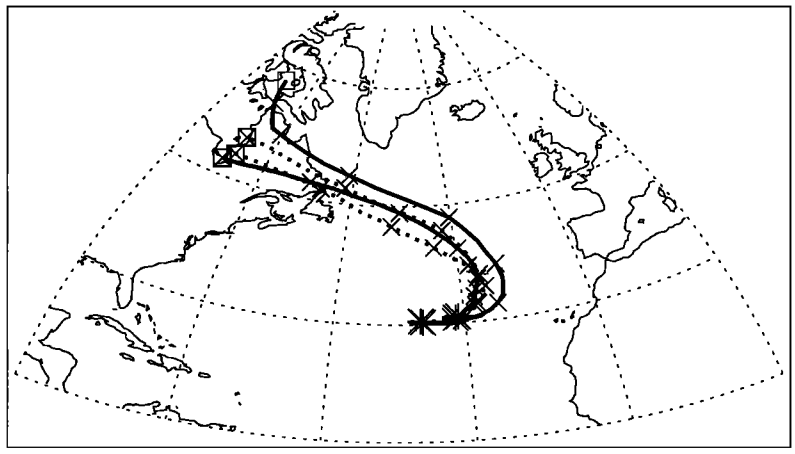

Figure 6. Back trajectories for June 5 through June 7, associated with I1 inhabited continental episode, JD 157.4-158.6.

instrument was down for most of this episode; however, there is a peak in both NO_2 and NOy near the end of the period. Back trajectories within the mixed layer trace to Europe, while those at 3-4 km have an origin in the North American continent. Mixed episode M6 followed a brief interruption of clean marine air (C6), JD 178.6-181.0 (June 26-28). Unfortunately, the chemical data for this time span were limited; the somewhat elevated (over background) levels of ozone did agree with the continental origin of most of the 2-km 10-day back trajectories.

Discussion

It is generally considered that ozone production in the troposphere is determined by the availability of NOx [*Crutzen,* 1970; *Fishman et al.,* 1979]. In several studies of the lower marine boundary layer in remote regions, a condition of net ozone destruction due to an insufficiency of NOx was reported [*Liu et al.,* 1983; *Chameides et al.,* 1987; *Thompson et al.,* 1993]. Other studies in areas more impacted by anthropogenic input have described regions of ozone production apparently extending into the marine boundary layer to considerable distances from the source areas, marked by elevated concentrations of ozone at sea level [*Oltmans and Levy,* 1992; *Savoie et al.,* 1992; *Parrish et al.,* 1992]. A principal goal of this study was to estimate the rates of ozone production and destruction in regions of the North Atlantic marine boundary layer sampled during the cruise. To that end, the time-dependent photochemical box model for atmospheric chemistry (PBMAC) was employed [*Yvon and Saltzman,* 1993]. Input into the model included relevant chemical and meteorological data obtained on board ship; parameters and concentrations not measured were computed; ozone production and destruction rates were then obtained from the sum of the various respective reaction rates, using the equations of *Liu et al.* [1992]. The model incorporates 160 reactions and 57 chemical species. Input parameters include temperature, total column ozone density, position, Julian day time, altitude, pressure, water vapor concentrations, alkenes, alkanes, NOx, CO, and O_3 concentrations. Photolysis rate constants were calculated from absorption cross sections and wavelength-dependent quantum yields data [*Finlayson-Pitts and Pitts,* 1986]. Actinic flux was calculated as the sum of direct and diffuse radiance by a two-stream radiation method

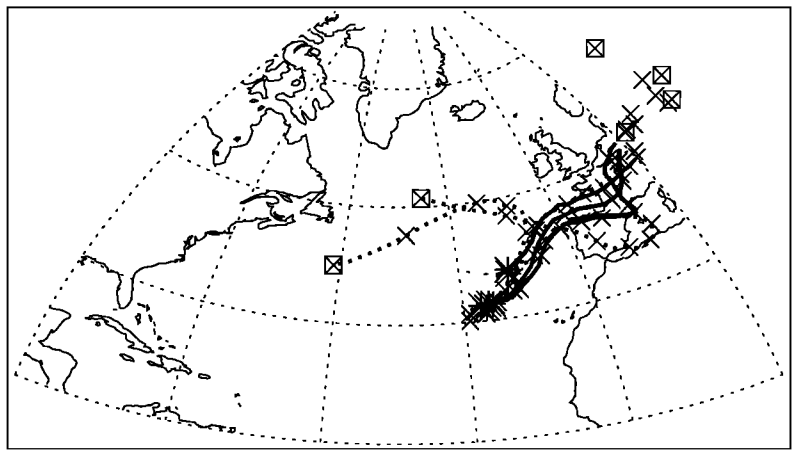

Figure 7. Back trajectories for June 17 through June 18, associated with I3 inhabited continental episode, JD 168.8-171.7.

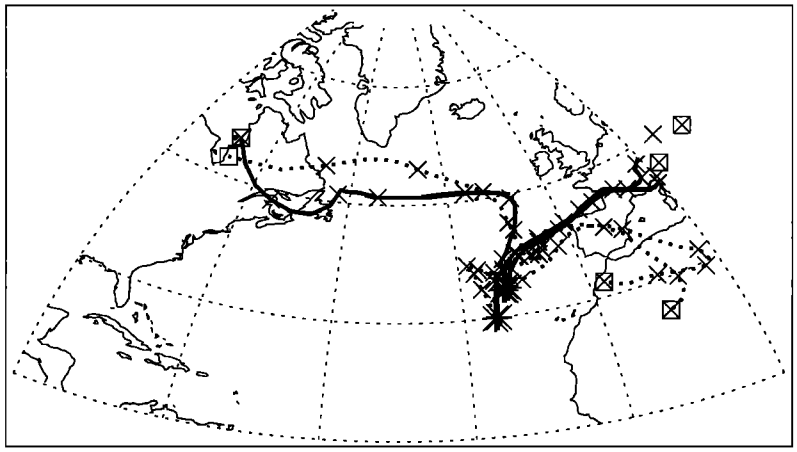

Figure 8. Back trajectories for June 20 through June 22, associated with I4 inhabited continental episode, JD 172.3-174.5.

[*Thompson,* 1984]. Reaction rates were taken from *NASA Panel for Data Evaluation* [1992] and other sources [*Yvon and Saltzman,* 1993]. A preliminary run list was generated using the Julian times of each NO/NO_2 measurement cycle. Concentrations of ozone, CO, UV, air temperature, and water vapor within +30 min of that time were averaged and held as fixed quantities during each run. If ozone or CO data within that time window were not available, that time was removed from the run list. For water vapor and temperature, a small number of measurements were missing or anomalous due to instrumental problems; for those cases, estimates from available data were used. Column ozone data were obtained from NASA for each day of the cruise; the geographically nearest TOMS value was extracted and used for individual runs. The solar zenith angle (computed from position and Julian time) was held constant during each run.

A total of 42 hydrocarbon samples were measured during the cruise. The concentrations of C_2H_2, C_2H_4, C_2H_6, C_3H_8, C_3H_6, and C_4H_8 were determined for each run time by interpolating between the concentrations obtained before and after that run time. The concentrations of $O(^1D)$, $O(^3P)$, CH_3, CH_3O_2, CH_3O, CHO, H, C_2H_5, $C_2H_5O_2$, $C_2H_5O_2H$, CH_2O_2, CH_2OHCH_2, CH_2OHCH_2O, $CH_2OHCH_2O_2$, CH_2OH, C_3H_7OO, CH_3CHO_2, alkane $-O_2$, and methyl ethyl keytone $-O_2$, were assumed to be in steady state equilibrium with the remaining species. No explicit C_5 or higher hydrocarbon chemistries were included. Deposition of ozone to the sea surface was assumed to be zero. For each set of initial conditions, the model was run for 168 hours (7 days) to attain near-steady state concentrations. A total of 62 runs with appropriate initial conditions were computed using the PBMAC program.

A list of typical initial conditions and starting concentrations is provided in Table 2. Quantities with asterisks in Table 2 were changed according to the measured values for that run; quantities without asterisks were fixed for all runs. The focus of the calculation was the determination of the net ozone production QO_3 (production rate minus destruction rate), principally determined by the key reactions R_1-R_6 [*Davis et al.,* 1996], where k_1-k_6 are the associated rate constants and brackets denote species concentration:

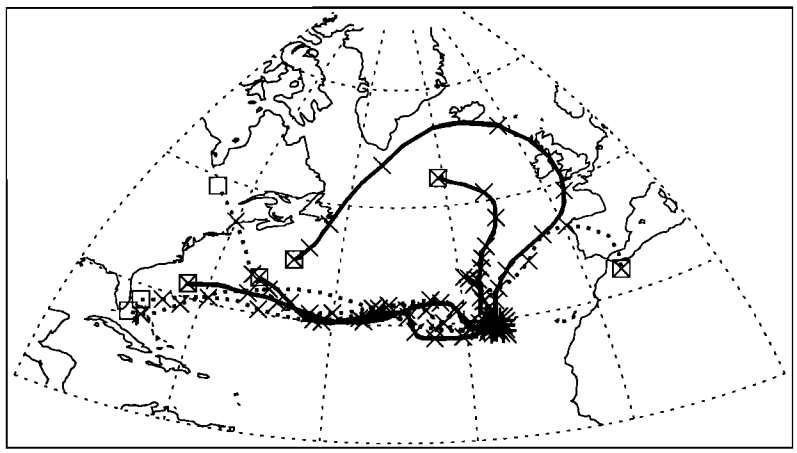

Figure 9. Back trajectories for June 22 through June 25, associated with M5 mixed marine/continental episode, JD 174.5-177.8.

Table 2. Input Parameters for PBMAC Model

Parameter	Value	Unites
Temperature*	22.47	°C
Column ozone*	321.	Dobson units
Latitude*	29.806	degrees, N positive
Longitude*	-47.00	degrees, E positive
Julian day*	156.0	
Atmospheric Pressure*	1.01	atmospheres
Water vapor*	17.17	g/kg
Relative Humidity*	77.94	%
Aerosol Surface Area	9.7	μmole m^{-2} cm^{-3}
Boundary Layer Height	1.4	km
Integration Time	168.0	hours (7 days)
Cloud base height	1.4	km
Surface albedo	0.07	
Methane	1.4	ppmv
CO*	130.8	ppbv
O_3*	29.43	ppbv
NO*	1.	pptv
NO_2*	49.	pptv
C_2H_2*	61	pptv
C_2H_6*	1.15	ppbv
C_2H_4*	136	pptv
C_3H_8*	362	pptv
C_3H_6*	199	pptv
C_4H_8*	84	pptv
$>C_3$ alkanes	50	pptv

* Changed for each individual run

R_1 $HO_2 + NO \rightarrow NO_2 + OH$
R_2 $CH_3O_2 + NO \rightarrow CH_3O + NO_2$
R_3 $C_2H_5O_2 + NO \rightarrow C_2H_5O + NO_2$
R_4 $O(^1D) + H_2O \rightarrow 2OH$
R_5 $HO_2 + O_3 \rightarrow OH + 2O_2$
R_6 $OH + O_3 \rightarrow HO_2 + O_2$

$$PO_3 = (R_1)[HO_2][NO] + (R_2)[CH_3O_2][NO] + (R_3)[C_2H_5O_2][NO] \quad (1)$$

$$DO_3 = (R_4)[H_2O][O(^1D)] + (R_5)[HO_2][O_3] + (R_6)[OH][O_3] \quad (2)$$

$$QO_3 = PO_3 - DO_3 \quad (3)$$

A plot of PO_3, DO_3, and QO_3 for JD 156 to 165 (June 4-13) is shown in Figure 10. Ozone production is dominated by (R_1) and destruction by (R_4) during the daytime. Ozone production generally matched destruction, with a net negative QO_3 for 16 out of 18 days, with QO_3 averaging -2.6×10^6 mol cm^{-3} s^{-1} or ~8 ppt d^{-1}. At night, ozone generation mechanisms remained small, with destruction via reaction (R_5) dominating. High NO during JD 159 and 163 led to reduced ozone destruction. No evidence of increased ozone generation at sunrise is evident. The sunrise maximum of ozone reported in the marine boundary layer [*Johnson et al.*, 1990; *Piotrowicz et al.*, 1989] was not unequivocally observed in this data set. Production did rise slightly with increasing NO concentration (Figure 11).

The runs in Figures 10 and 11 contain episodes of clean, mixed, and inhabited continental air; however, the calculated value of QO_3 was generally not a strong function of airmass origin. The $\Delta O_3/\Delta CO$ ratios were computed using the reduced major axis method [*Sokal and Rohlf*, 1981] from ozone measurements averaged over ±10 min of each CO measurement (Figure 12). The ratio for the clean marine episode, 0.24, was similar to ratios from reported by *Parrish et al.* [1993] of 0.22-0.27 and *Dickerson et al.* [1995] of 0.27. The I and M categories had substantially higher ratios of 0.70 to 0.79, indicating additional photochemical processing of the continental air. The highest ratio was from the U category; this may be due to faster removal of CO compared to O_3 for these airmasses.

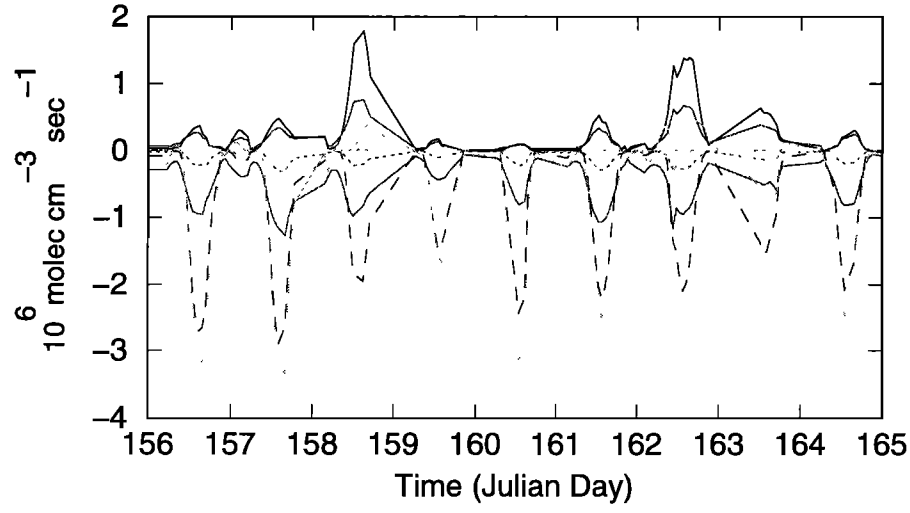

Figure 10. Reaction rates for individual ozone production and destruction reactions during JD 156-165 (June 4-13, 1992). O_3 production reactions (above zero) are (R_1) (solid line), (R_2) (dotted line), and (R_3) (dashed line); destruction reactions (below zero) are (R_4) (solid line), (R_5) (dotted line), and (R_6) (dashed line). Net QO_3 is given by the spike.

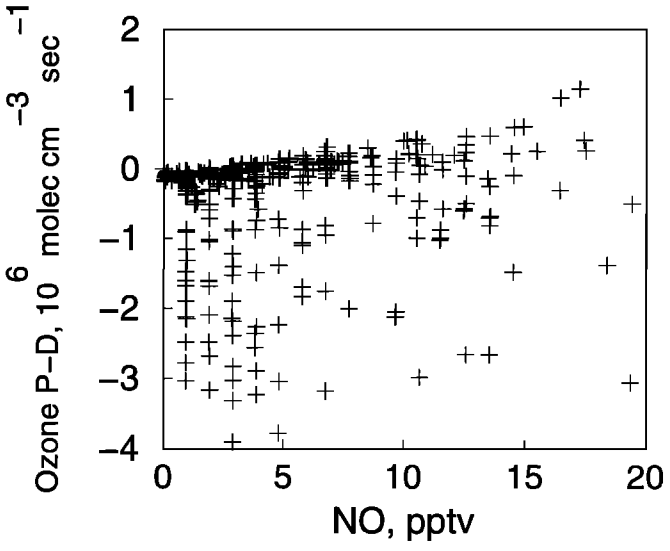

Figure 11. Net ozone production (QO_3) versus NO concentration for each of the 62 runs.

Conclusions

From an analysis of the chemical, meteorological and trajectory data from the cruise, specific episodes in which plumes of continentally influenced air as well as intervals of generally clean marine air were identified. Concentrations of key species in clean episodes exceeded background concentrations measured in the remote Pacific and in the South Atlantic.

Using chemical and meteorological data obtained near sea level in the North Atlantic in a simple one-dimensional photochemical model, it was found that ozone destruction predominated over generation. The principal source of ozone destruction was removal of $O(^1D)$ by water vapor.

In most cases, O_3/CO ratios exceeded the ratio of ~0.3 which has been noted for regions dominated by processes characteristic of eastern seaboard North America. The higher ratios were interpreted as indications of greater photochemical processing of these airmasses.

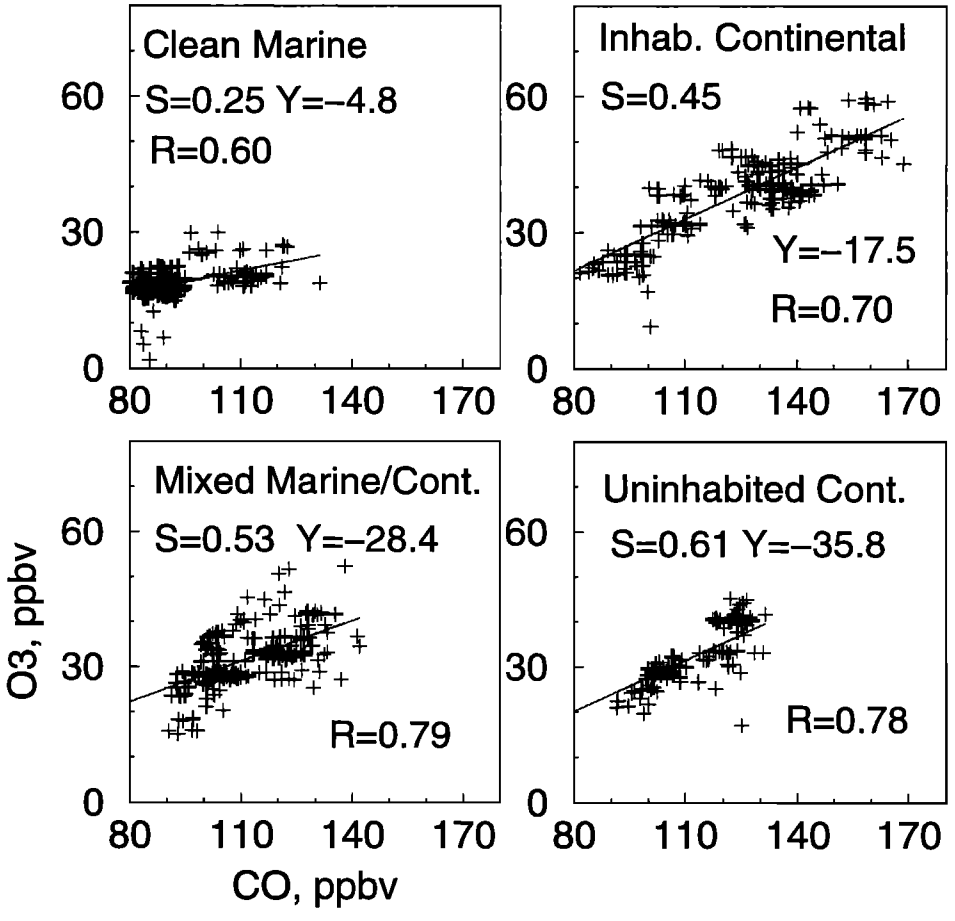

Figure 12. Ozone versus CO data for the individuual airmass types. Each data point represents a CO measurement and an average of the ozone measurements within ±10 min. Overall slope from all data JD 156-181 was 0.47.

Acknowledgments. The authors would like to thank the officers and crew of the R/V *Malcolm Baldrige* for providing the platform for these investigations. Additionally, we would like to thank G. Variot for operation of the aethalometer and radon systems, Lieutenant M. Robinette, J. Cione and S. Piotrowicz for rawinsonde operations and back trajectory calculations.

References

Ancellet, G., M. Beekmann, and A. Papayannis, Impact of a cutoff low development on downward transport of ozone in the troposphere, *J. Geophy. Res., 99*, 3451-3468, 1994.

Bachmeier, A. S., M. C. Shipham, E. V. Browell, W. B. Grant, and J. M. Klassa, Stratospheric/tropospheric exchange affecting the northern wetlands region of Canada during summer 1990, *J. Geophy. Res., 99*, 1793-1804, 1994.

Bamber, D. J., P. G. W. Healey, B. M. R. Jones, S. A. Penkett, and A. F. Tuck, Vertical profiles of tropospheric gases: Chemical consequences of stratospheric intrusions, *Atmos. Environ. 18*, 1759-1766, 1984.

Bateman, H., Solution of a system of differential equations in the theory of radio-active transformations, *Proc. Cambridge Philos. Soc., 15*, 423, 1910.

Broll, A., G. Helas, K.-J. Rumpel, and P. Warneck, NOx background mixing ratios in the surface air over Europe and the Atlantic Ocean, in *Physico-Chemical Behaviour of Atmospheric Pollutants*, edited by B. Versino and G. Angeletti, pp. 390-400, D. Reidel, Norwell, Mass., 1990.

Carney, T. A., and J. Fishman, A one-dimensional photochemical model of the troposphere with a trade-wind boundary-layer parameterization, *Tellus, 38B*, 112-143, 1986.

Carroll, M. A., M. McFarland, B. A. Ridley, and D. L. Albritton, Ground-based nitric oxide measurements at Wallops Island, Virginia, *J. Geophys. Res., 90*, 12,853-12,860, 1985.

Chameides, W. L., D. D. Davis, M. O. Rodgers, J. Bradshaw, S. Sandholm, G. Sachse, G. Hill, G. Gregory, and R. Rasmussen, Net ozone photochemical production over the eastern and central North Pacific as inferred from GTC/CITE 1 observations during fall 1983, *J. Geophys. Res., 92*, 2131-215, 1987.

Crutzen, P. J., The influence of nitrogen oxides on the atmospheric ozone content, *Q. J. R. Meteorol. Soc., 96*, 320-325, 1970.

Crutzen, P. J., The role of NO and NO_2 in the chemistry of the troposphere and stratosphere, *Annu. Rev. Earth Planet. Sci., 7*, 443-472, 1979.

Davis, D. D., *et al*, Assessment of ozone photochemistry in the western North Pacific as inferred from PEM-West A observations during the fall 1991, *J Geophys. Res., 101*, 2111-2134, 1996.

Dickerson, R. R., B. G. Doddridge, K. P. Rhoads, and P. Kelley, Large-scale pollution of the atmosphere over the remote Atlantic Ocean: Evidence from Bermuda, *J. Geophys. Res., 100*, 8945-8962, 1995.

Doddridge, B. G., P. A. Dirmeyer, J. T. Merrill, S. J. Oltmans, and R. R. Dickerson, Interannual variability over the eastern North Atlantic Ocean: Chemical and meteorological evidence for tropical influence on regional-scale transport in the extratropics, *J. Geophys. Res., 99*, 22,923-22,935, 1994.

Draxler, R. R., Hybrid single-particle Lagrangian integrated trajectories (Hy-Split): Version 3.0--User's guide and model description, *NOAA Tech. Memo., ERL ARL-195*, 1992.

Fehsenfeld, F. C., R. R. Dickerson, G. Hubler, J. G. Calvert, and B. A. Ridley, A ground-based intercomparison of NO, NOx, and NOy measurement techniques, *J. Geophys. Res., 92*, 14,710-14,722, 1987.

Finlayson-Pitts, B. J., and J. N. Pitts Jr., *Atmospheric Chemistry: Fundamentals and Experimental Techniques*, 1098 pp., John Wiley, New York, 1986.

Fishman, J., S. Solomon, and P. J. Crutzen, Observational and theoretical evidence in support of a significant in-situ photochemical source of tropospheric ozone, *Tellus, 31*, 423-446, 1979.

Goldberg, E. D., *Black Carbon in the Environment*, 196 pp., John Wiley, New York, 1985.

Hansen, A. D. A., R. S. Artz, A. A. P. Pszenny, and R. E. Larsen, Aerosol black carbon and radon as tracers for airmass origin over the North Atlantic Ocean, *Global Biogeochem. Cycles, 4*, 189-199, 1990.

Holton, J. R., *An Introduction to Dynamic Meteorology*, 3rd ed., 509 pp., Academic, San Diego, Calif., 1992.

Houghton, H. G., *Physical Meteorology*, 442 pp., MIT Press, Cambridge, Mass., 1985.

Jenkins, R., *X-Ray Fluorescence Spectrometry*, p. 187, Am. Chem. Soc., Washington, D.C., 1978.

Johnson, J. E., R. H. Gammon, J. Larsen, T. S. Bates, S. J. Oltmans, and J. C. Farmer, Ozone in the marine boundary layer over the Pacific and Indian Oceans: Latitudinal gradients and diurnal cycles, *J. Geophys. Res., 95*, 11,847-11,856, 1990.

Joseph, D. W., and C. W. Spicer, Chemiluminescence method for atmospheric monitoring of nitric acid and nitrogen oxides, *Anal. Chem., 50*, 1400-1403, 1978.

Kasibhatla, P. S., H. Levy II, and W. J. Moxim, Global NOx, HNO3, PAN, and NOy distributions from fossil fuel combustion emissions: A model study, *J. Geophys. Res., 98*, 7165-7180, 1993.

Larson, R. E., and D. J. Bressan, Automatic radon counter for continual unattended operation, *Rev. Sci. Instrum., 49*, 965-959, 1978.

Levy, H., J. D. Mahlman, and W. J. Moxim, A stratospheric source of reactive nitrogen in the unpolluted troposphere, *Geophys. Res. Lett., 7*, 441-444, 1980.

Liu, S. C., M. McFarland, D. Kley, O. Zafiriou, and B. Huebert, Tropospheric NOx and O_3 budgets in the equatorial Pacific, *J. Geophys. Res., 88*, 1360-1368, 1983.

Liu, S. C., M. Trainer, F. Fehsenfeld, D. Parrish, E. Williams, D. Fahey, G. Hubler, and P. Murphy, Ozone production in the rural troposphere and the implications for regional and global ozone distributions, *J. Geophys. Res., 92*, 4191-4207, 1987.

Liu, S. C., M. Trainer, M. A. Carroll, G. Hubler, D. D. Montzka, R. B. Norton, B. A. Ridley, J. G. Walega, E. L. Atlas, B. G. Heikes, B. J. Huebert, and W. Warren, A study of the photochemistry and ozone budget during the Mauna Loa Observatory Photochemistry Experiment, *J. Geophys. Res., 97*, 10,463-10,471, 1992.

NASA Panel for Data Evaluation, Chemical kinetics and photochemical data for use in strospheric modeling, Eval. 10, *JPL Publ. 92-20*, Jet Propul. Lab., Calif. Inst. of Technol., Pasadena, 1992.

Novelli, P. C., L. P. Steele, and P. P. Tans, Mixing ratios of carbon monoxide in the troposphere, *J. Geophys. Res., 97*, 20,731-20,750, 1992.

Oltmans, S. J., and H. Levy II, Seasonal cycle of surface ozone over the western North Atlantic, *Nature, 358*, 392-394, 1992.

Parrish, D. D., C. J. Hahn, F. C. Fehsenfeld, H. B Singh, and B. A. Ridley, Indications of photochemical histrories of Pacific airmasses from measurements of atmospheric trace species at Point Arena, California, *J. Geophys. Res., 97*, 15,883-15,901, 1992.

Parrish, D. D., J. S. Holloway, M. Trainer, P. C. Murphy, G. L. Forbes, and F. C. Fehsenfeld, Export of North American ozone pollution to the North Atlantic Ocean, *Science, 259*, 1436-1439, 1993.

Piotrowicz, S., R. Rasmussen, K. Hanson, and C. Fischer, Ozone in the boundary layer of the equatorial Atlantic Ocean, *Tellus, 41B*, 314-322, 1989.

Piotrowicz, S. R., C. J. Fischer, and R. S. Artz, Ozone and carbon monoxide over the North Atlantic during a boreal summer, *Global Biogeochem. Cycles, 4*, 215-224, 1990.

Ridley, B. A., Measurements of minor constituents in the stratosphere by chemiluminescence, *Atmos. Tech., 9*, 27-34, 1978.

Rohrer, F., and D. Brüning, Surface NO and NO_2 mixing ratios

measured between 30°N and 30°S in the Atlantic region, *J. Atmos. Chem., 15,* 253-267, 1992.

Savoie, D. L., J. M. Prospero, S. J. Oltmans, W. C. Graustein, K. K. Turkekian, J. T. Merrill, and H. Levy II, Sources of nitrate and ozone in the marine boundary layer of the tropical North Atlantic, *J. Geophys. Res., 97,* 11,575-11,589, 1992.

Sokal, R. R., and F. J. Rohlf, *Biometry,* 2nd ed., W. H. Freeman, New York, 1981.

Thompson, A. M., The effect of clouds on photolysis rates and ozone formation in the unpolluted troposphere, *J. Geophys. Res., 89,* 1341-1349, 1984.

Thompson, A. M., *et al.,* Ozone observations and a model of marine boundary layer photochemistry during SAGA 3, *J. Geophys. Res., 98,* 16,995-16,968, 1993.

Wilkening, M. H., and W. E. Clements, Radon 222 from the ocean surface, *J. Geophys. Res., 80,* 3828-3830, 1975.

Winkler, P., Surface ozone over the Atlantic Ocean, *J. Atmos. Chem., 7,* 73-91, 1988.

Yvon, S., and E. Saltzman, A time-dependent photochemical box model for atmospheric chemistry (PBMAC), *Tech. Rep. RSMAS-TR-93-008,* Rosenstiel School of Mar. and Atmos. Sci., Univ. of Miami, Miami, Fla., 1993.

B. Bonsang, Centre des Faibles Radioactivités, Centre National de la Recherche Scientifique, 91198 Gif sur Yvette, France.

T. P. Carsey, M. L. Farmer, C. J. Fischer, and M. Springer-Young, National Oceanic and Atmospheric Administration, Atlantic Oceanographic and Meteorological Laboratory, 4301 Rickenbacker Causeway, Miami, FL 33149. (e-mail: carsey@aoml.noaa.gov).

D. D. Churchill and E. S. Saltzman, Rosenstiel School of Marine and Atmospheric Science, University of Miami, 4600 Rickenbacker Causeway, Miami, FL 33149.

A. A. Pszenny, IGAC Office, Department of Chemistry, Massachusetts Institute of Technology, Cambridge, MA 02139.

V. B. Ross, U.S. Navy, PSC 804 Box 10, FPO, AE 09409-1010.

(Received September 21, 1994; revised July 12, 1996;
accepted October 17, 1996.)